ADVANCED OPTICAL MATERIALS

www.advopticalmat.de

# Controlling the Color of Plasmonic Substrates with Inkjet Printing

*Luc Duempelmann, Judith A. Müller, Fabian Lütolf,* Benjamin Gallinet, Rolando Ferrini, and Lukas Novotny*

**This study introduces a versatile method for modifying the optical properties of plasmonic substrates by inkjet printing of commercially available, transparent inks with various refractive indices. The large-scale and cost-efficient process is demonstrated on tilted aluminum nanolamellas. They show vivid and bright colors based on a Fano resonance, which is highly susceptible to the surrounding material. Furthermore, color rendering can be made strongly angle-dependent and asymmetric, which is in contrast to the nonvariable color generation enabled by conventional inkjet printing.**

## 1. Introduction

Metallic nanostructures can strongly interact with visible light.[1] These so-called plasmonic color substrates can be composed of, e.g., nanodisks,[2,3] nanopatches,[4,5] or metal–insulator–metal nanoresonators.[6] The underlying plasmonic resonance can depend on the geometry of the structure,[2–4] the viewing angle,[7–9] and polarization[5,6,10,11] of the incident light or on the refractive index (RI) of the surrounding.[1] The latter can be exploited for biosensing[12] or recently for color generation.[13] Lately, plasmonic substrates were fabricated with the abundant and complementary metal oxide semiconductor (CMOS) compatible aluminum[14,15] in upscalable, cost-efficient processes, paving the way toward industrial manufacturing.[3,4,9]

Currently, there is great interest in customized, affordable, and rapid color printing with active variable and controlled optical appearance,[10,11,13,15] e.g., optical security[7,8,16] or imaging applications.[17,18] To date, replication of microscopic patterns consisting of nanostructures often requires a lithographically defined master structure, which is complex and expensive to fabricate (e.g., e-beam) and cannot be adapted in a simple manner.[19] Alternatively, plasmonic structures can be modified with a laser writing process at high resolution.[15] On the other hand, conventional inkjet printing techniques offer customized color generation and therefore belong to the most common processes in the graphic industry.[20] Typical coloration is based on chemical dyes or pigments that are prone to photobleaching and smearing when coming into contact with water or grease.[21] Novel techniques allow printing of, e.g., quantum dots[22] or nanocrystals.[23] Although such color generating structures can be printed below the diffraction limit,[24] the used inks are highly specialized or have limited lifetimes. In addition, such techniques are often severely limited in printing speed,[24] require special dispensing techniques[23] or accurate control over the thickness of the dispensed material.[25] Finally, the color appearance is either nonvariable (quantum dot)[22] or iridescent (interference).[25] For a wide range of consumer applications, nonvariable colors could be fabricated with conventional inkjet printing instead. It is further difficult to recognize a clear image of iridescent patterns, which finally are also often perceived as outdated for security applications.

Here, we present an approach for customizing the optical properties of plasmonic substrates via inkjet printing. Plasmonic substrates, which are sensitive to the RI, are used as a cost-efficient, adaptable, and versatile basis, while inkjet printing allows the pixelwise control over the resulting colors. A standard desktop printer without modifications is used to dispense transparent and commercially available inks with different refractive indices (RI-ink). In particular, we use plasmonic substrates consisting of tilted aluminum nanolamellas. The optical appearance is based on a Fano resonance, which is strongly modified by the RI, enabling printed pixels with an ink-dependent color effect. Further, the structures show an angle-dependent and asymmetric color appearance, which can be varied by the viewing angle. Such variable and controlled optical appearance, not achievable with conventional inkjet printing, paves the way toward individualized color filters, which are sought-after in optical security, for decorative elements or camera applications.

## 2. Results and Discussion

**Figure 1** shows the process scheme for inkjet printing on plasmonic substrates. The plasmonic substrate is fabricated by

L. Duempelmann, J. A. Müller, Dr. F. Lütolf, Dr. B. Gallinet, Dr. R. Ferrini
Thin Film Optics
CSEM SA
Tramstrasse 99, 4132 Muttenz, Switzerland
E-mail: fabian.luetolf@csem.ch
L. Duempelmann, Prof. L. Novotny
Department of Information Technology and Electrical Engineering (D-ITET)
ETH Zurich
Gloriastrasse 35, 8092 Zürich, Switzerland
The ORCID identification number(s) for the author(s) of this article can be found under http://dx.doi.org/10.1002/adom.201700153.

**DOI: 10.1002/adom.201700153**

 

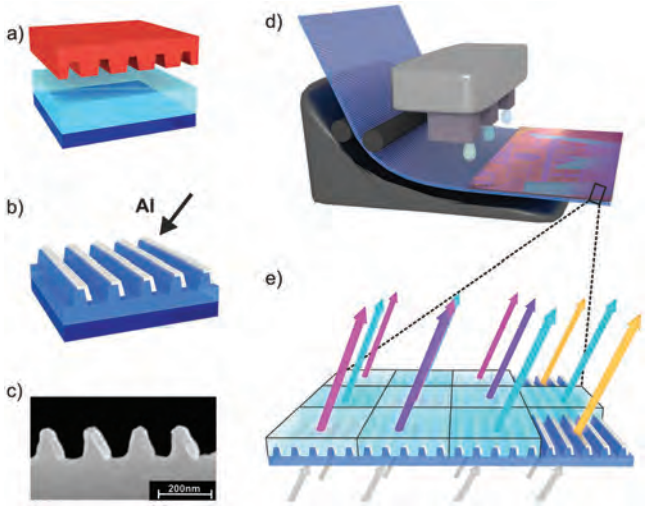


**Figure 1.** Fabrication scheme including: a) nanoimprint lithography with a master and b) angular evaporation of aluminum leading to a large-scale and flexible plasmonic foil. c) Scanning electron microscopy (SEM) image of the evaporated structure. d) Subsequent inkjet printing of transparent RI-inks onto the substrate. e) Scheme of the pixelized color generation under tilted illumination. Photograph: Norbert Aepli.

replication of a periodic pattern into UV curable material on a flexible polyethylene teraphthalate (PET) foil and subsequent evaporation of aluminum at an oblique angle, see Figure 1a–c. Finally, inkjet printing of transparent RI-inks onto the uniform plasmonic foil locally alters the plasmon resonance, which gives each pixel a distinct optical appearance, see Figure 1d,e. Due to the geometrical asymmetry, the optical appearance is pronounced at a tilt angle. Optionally, to circumvent abrasion, an additional low RI material with high viscosity can be applied for protection via spin coating, see Figure S1 (Supporting Information).

The aluminum nanolamellas reveal a characteristic Fano-like line shape that originates from strong coupling between a localized surface plasmon resonance (LSPR) and a propagating resonance (PR).[9] **Figure 2**a shows the transmission of the structure at an incidence angle $\theta = -60°$. While the LSPR is a feature of the geometry of the individual plasmonic resonators (e.g., tunable via evaporation angle), the PR is influenced by their periodic arrangement. Both resonances are susceptible to the RI of the surrounding.[1] While the RI of the surrounding coating ($n_{coat}$) can be varied by inkjet printing (RI-ink), the RI of the supporting substrate ($n_{sub}$) remains constant (see scheme, Figure 2a). A spectral signature of the PR is the Wood–Rayleigh anomaly (WR).[26] The position can be calculated by $\lambda_R = p(\sin(\theta) + n)$,[27] with the period $p$ and the refractive index $n$ of the media. The presence of two dielectric materials leads to a $WR_{coat}$ of the coating and a $WR_{sub}$ of the substrate (solid and dashed black line in Figure 2). The spectral position of the LSPR depends on the ratio of $n_{coat}$ to $n_{sub}$ (filling ratio) in the plane of the plasmonic structures (see schemes, Figure 2b). While the position changes nearly 290 nm per refractive index unit (RIU) for structures surrounded by mainly $n_{coat}$ (blue, Figure 2b), it shifts only ≈70 nm per RIU for structures surrounded by mainly $n_{sub}$ (green, Figure 2b). Ultimately there is a trade-off between color shifting capability (see color bars, Figure 2b) and ease of fabrication. We used a geometry with a relatively high susceptibility of ≈160 nm per RIU (red, Figure 2a,b), which remains reasonably easy to fabricate. The strong dependence of the LSPR on $n_{coat}$ can be explained with a high near-field enhancement between the nanolamellas,[9] enhancing the interaction with the enclosed material. This is likely linked to the in-plane propagation of the PR.

In conclusion, both spectral features respond to the RI of the surrounding. While the position of the LSPR can be modified by the filling factor (Figure 2b), the position of the WR is altered by the period (Figure S2, Supporting Information) and the incident angle $\theta$ (**Figure 3**). Close proximity of the two resonances can lead to a Fano-like line shape by strong coupling.[9] A spectral shift (e.g., induced by different RI) of such a pronounced resonance leads to a great color change and therefore distinct perception, in contrast to broad resonances. For the proposed tilted structure such strong coupling in particular is the case at an incidence angle of $\theta = -60°$, see Figures 2 and 3.

Figure 3 shows the angle-dependent transmission plots for the plasmonic substrates bearing different $n_{coat}$. With steeper angle (toward 0°), the WR's (gray cross and dashed line) shift to the blue (see equation). Additionally, the strength of the LSPR (orange plus) decreases with increasing angles due to the tilt of the plasmonic structure. These effects lead to a flattening of the Fano-like line shape, hence, to an asymmetric color generation (see color bars), also reported elsewhere.[9] Finally, as discussed for Figure 2, the RI of the coating strongly changes the position and shape of the coupled resonances, leading to distinct color generation (color bars) at negative angles. The agreement between measurements and simulation is very good.

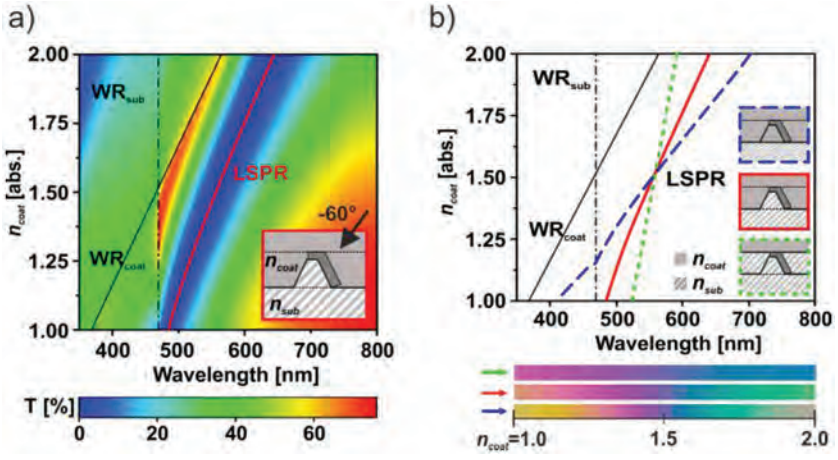


**Figure 2.** a) Simulated transmission spectra as a function of $n_{coat}$ at $\theta = -60°$. b) Corresponding spectral position of the LSPR's (at minimum position) for different filling of the structures (see scheme), including the $WR_{coat}$ and $WR_{sub}$. The color bars below indicate the corresponding color.

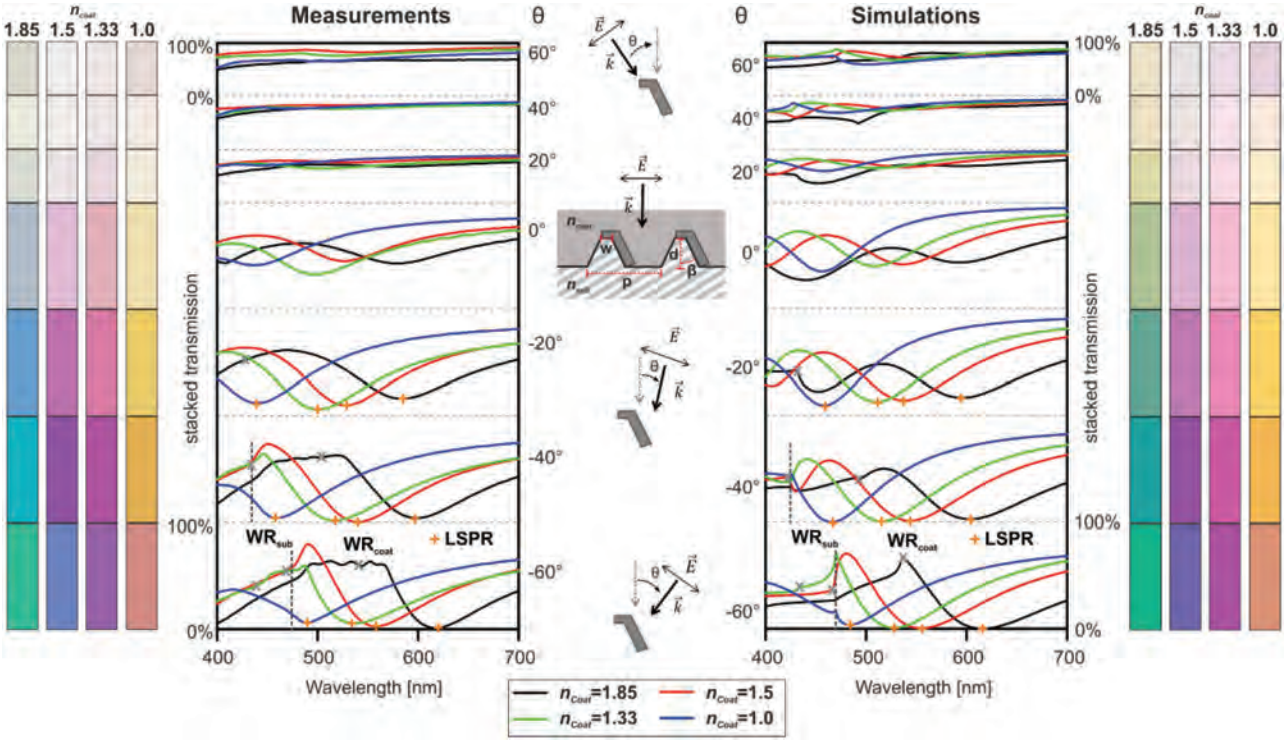


**Figure 3.** Transmission spectra of TM-polarized light for different angles of incidence $\theta$ and $n_{coat}$ (colored lines). Measurements are shown on the left and simulations on the right. Observed colors at the corresponding angles are given next to the graphs. $WR_{coat}$: gray cross, $WR_{sub}$: dashed line, LSPR: orange plus. The sketches in the middle illustrate the orientation of the electric field $E$, the wavevector $k$, and the angle $\theta$ in respect to the nanolamellas, with $p$ = 200 nm, d = 120 nm, w = 35.5 nm, $\beta$ = 18° and thickness of aluminum = 13 nm.

The RI- and angle-dependence is further depicted in **Figure 4**. The transmitted color is computed ($n_{coat}$ = 1.0–2.0, white lines) and measured (different RI-inks, black cross) for $\theta$ = –60° and +40°. At positive angles, almost perfect color neutrality ($w$) is observed, whereas at negative angles distinct vivid colors are visible. The circular arrangement indicates the wide range of colors available with the presented method, even exceeding the CMYK color range. Besides the measured four colors (crosses), more colors can be obtained by printing adjacent pixels with distinct RI-inks. This color mixing is similar to pigment mixing with a conventional inkjet printer. Adjusting the ratio of the RI-inks generates the colors enclosed by these four points (see Figure S3, Supporting Information). Alternatively, it is possible to generate the colors along the circle, by using inks with the appropriate RI or actual mixing of RI-inks. The latter would strongly enhance the range of possible colors, which can be printed with only two inks of very low and very high RI. Finally, the attainable color range (as shown in Figure 4) is defined by the characteristics of the plasmonic structure, which could be altered to address different color ranges.[9]

The used plasmonic structures are ideal candidates for the asymmetric and RI-dependent color generation due to the tilt of the nanolamellas, arranged on a small structural support ($n_{sub}$), respectively. Nevertheless, the proposed method could be applied for a large variety of plasmonic structures. To demonstrate this, we used and replicated nonideal, but relatively cost-efficient and readily available nanostructures, see **Figure 5**d. After angular evaporation of aluminum, an image with different

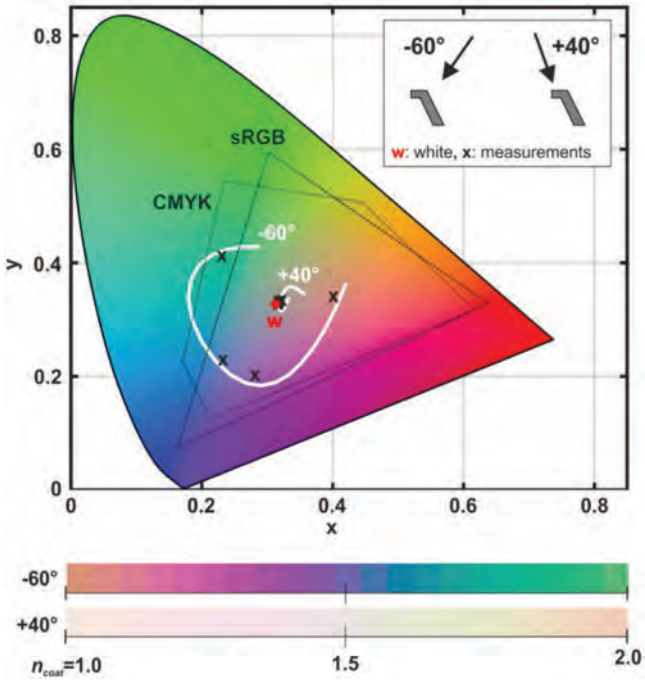


**Figure 4.** CIE color plot with $n_{coat}$ between 1.0 and 2.0 (white line, color bar below) and $\theta$ = –60° and +40°. The measured samples (black cross), and the CMYK and sRGB color ranges are indicated.

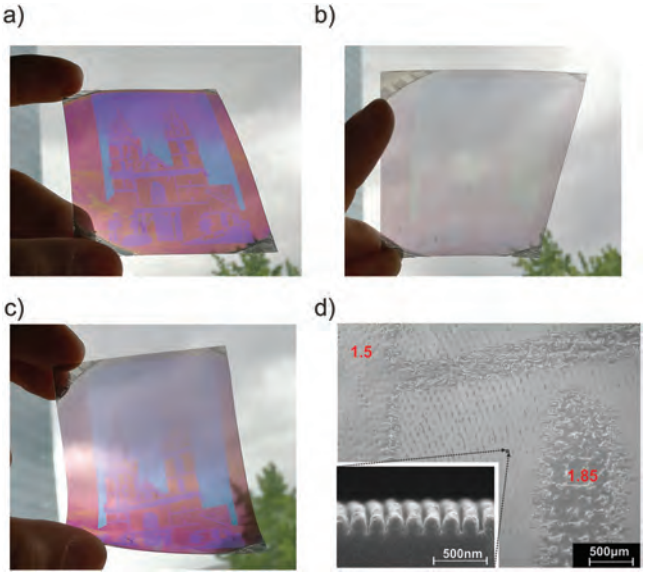


**Figure 5.** a–c) Images of a printed sample (5 × 6 cm) at different viewing angles with color generation only upon certain tilt angles. Photographs were taken in front of a cloudy sky and with unpolarized light. d) SEM of replicated nanostructures (bottom left) and light microscope image of an inkjet printed sample. The numbers indicate the RI of the ink. Photograph: Nobert Aepli.

RI-inks was inkjet-printed (effect illustrated in Figure S4, Supporting Information). Clearly, the image and its different colors are only visible upon one tilt direction (Figure 5a,b), highlighting the optical symmetry breaking effect. Such hidden features are highly attractive for optical security applications. Further, a bending of the foil leads to color generation only in parts of the sample (Figure 5c). The optical appearance is only governed by light directly transmitting through the sample, so-called zero order. This enables its use in diffuse light (e.g., cloudy sky). By contrast, diffractive structures would lead to an overlay of light from different parts of the sample, creating a faint or unclear image. Furthermore, the colors could rapidly change with viewing angle. This makes a clear recognition of the optical image more difficult. By contrast, Figure 5c shows that bending of the sample renders a relative stable hue, while mainly changing the saturation.[28] Finally, it is important to note that the plasmonic resonance is only excited with transverse magnetic (TM) polarized light; with transverse electric (TE) polarized light almost no optical features are observed.[9] Since the plasmon resonance is so pronounced, color generation is clearly visible even in the unpolarized light used here. Besides, the thin layer of aluminum shows high transmission values allowing bright and vivid colors.

## 3. Conclusion

We demonstrate a wide range of vivid and bright colors achieved with inkjet-printed plasmonic structures. While uniform aluminum plasmonic substrates can be fabricated in a cost-efficient roll-to-roll compatible process, inkjet printing enables their customized modification. This proposed method could be seen as an alternative to "plasmonic laser printing."[29] Compared to conventional dyes or other inkjet printing techniques, e.g., quantum dots, plasmonic colors can show variable and novel optical appearances. Such customized and variable optical effects are highly desired in applications, such as optical security[7,8] or decorative elements, but also for camera applications.[17,18] Besides transmission, such printable color generation is also observed in reflection. Finally, the flexibility of the plasmonic foil offers exciting opportunities for novel applications.[30]

A greater palette of colors can be achieved by printing adjacent colored pixels, in situ mixing of different refractive index inks or by extending the range of available inks and plasmonic substrates. Simulations showed that the utilized resonances and corresponding printed inks could be adapted to be active in other spectral regimes, e.g., near-infrared.[9] Further, alternative plasmonic structures (e.g., nanodisks[2]) with distinct optical effects[15] could be customized with the proposed method. Besides a sensitivity of the plasmonic structure to the refractive index of the surrounding, we do not see any further requirements or adaptions necessary to use the proposed method directly with other structures potentially fabricated in a roll-to-roll compatible process.[29,31] Using inkjet printers with a smaller dispensing volume, e.g., NanoDrip,[22] could strongly increase the spatial resolution of the plasmonic color printing. Finally, the fabricated structures are nonorganic and can be well protected, therefore are not subjected to abrasion, oxidation, smearing, or UV degradation, such as conventional colors.[32]

## 4. Experimental Section

*Fabrication*: A master structure was fabricated using immersed laser interference lithography as described by Duempelmann et al.[9] Replication was done with Lumogen (BASF) and 50 s of UV exposure (Suess Mircotech, 1000 W Hg lamp) on top of a PET foil. Aluminum (8 nm) was evaporated with an electron beam evaporator. A commercially available inkjet printer (Epson, WF-2010) was used to dispense commercial inks with $n$ = 1.85 and 1.5 on the plasmonic substrate without further surface modification. We used a UV curable ink based on $TiO_2$ particles and a polymeric matrix to reach a nominal $n$ = 1.85, whereas the $n$ = 1.5 ink is purely polymeric and also UV curable. Their respective viscosities are around 5 mPa·s and 15 mPa·s. The inks can be diluted in isopropanol or ethanol to lower their solid content and viscosity. Optionally, a low refractive index material with $n$ = 1.33 was spin coated. The final device shown in Figure 5 was made by replication of readily available nanostructures (5 × 6 cm, period: 180 nm, duty cycle: 0.5, rectangular profile) and printing the image with a resolution of 600 dpi. The photos were taken in unpolarized light in front of a cloudy sky.

*Characterization*: The transmission measurements were done with a spectrometer (Perkin Elmer, Lambda 9) and a Glenn-Thomson polarizer. The illumination spot was about 3 × 5 mm. A home-made Matlab script (version 2015) was used to transfer the measured transmission values into RGB values.

*Computations*: Computations were done with rigorous coupled-wave analysis[33] in the range of 400–700 nm, in 2 nm steps. The angle of the zero order transmission was varied from $\theta$ = –60° to 60° in 20° steps and varying refractive index of $n$ = 1.00–2.00 in 0.05 steps. Hereby we assumed a constant refractive index over all wavelengths ($n(\lambda) = n$). A CIE (Commission internationale de l'éclairage) color plot (CIE 1931 color space)[28] including the range of sRGB (standard: IEC 61966-2-1:1999) and CMYK (profile: U.S. Web Coated SWOP v2) was used to plot the simulated color values.

## Supporting Information

Supporting Information is available from the Wiley Online Library or from the author.

## Conflict of Interest

The authors declare no conflict of interest.

## Keywords

aluminum structures, inkjet printing, plasmonic color substrates, refractive index inks, symmetry breaking

Received: February 16, 2017
Revised: March 16, 2017
Published online:

[1] L. Novotny, B. Hecht, *Principles of Nano-Optics*, Cambridge University Press, Cambridge, UK, **2012**.
[2] K. Kumar, H. Duan, R. S. Hegde, S. C. W. Koh, J. N. Wei, J. K. W. Yang, *Nat. Nanotechnol.* **2012**, *7*, 557.
[3] J. S. Clausen, E. Højlund-Nielsen, A. B. Christiansen, S. Yazdi, M. Grajower, H. Taha, U. Levy, A. Kristensen, N. A. Mortensen, *Nano Lett.* **2014**, *14*, 4499.
[4] J. Olson, A. Manjavacas, L. Liu, W. S. Chang, B. Foerster, N. S. King, M. W. Knight, P. Nordlander, N. J. Halas, S. Link, *Proc. Natl. Acad. Sci. USA* **2014**, *111*, 14348.
[5] V. R. Shrestha, S.-S. Lee, E.-S. Kim, D.-Y. Choi, *Nano Lett.* **2014**, *14*, 6672.
[6] T. Xu, Y.-K. Wu, X. Luo, L. J. Guo, *Nat. Commun.* **2010**, *1*, 59.
[7] J. Sauvage-Vincent, S. Tonchev, C. Veillas, S. Reynaud, Y. Jourlin, *J. Eur. Opt. Soc.* **2013**, *8*, 13015.
[8] H. Lochbihler, *Adv. Opt. Technol.* **2015**, *4*, 71.
[9] L. Duempelmann, D. Casari, A. Luu-Dinh, B. Gallinet, L. Novotny, *ACS Nano* **2015**, *9*, 12383.
[10] X. M. Goh, Y. Zheng, S. J. Tan, L. Zhang, K. Kumar, C.-W. Qiu, J. K. W. Yang, *Nat. Commun.* **2014**, *5*, 1.
[11] L. Duempelmann, A. Luu-Dinh, B. Gallinet, L. Novotny, *ACS Photonics* **2016**, *3*, 190.
[12] A. A. Yanik, A. E. Cetin, M. Huang, A. Artar, S. H. Mousavi, A. Khanikaev, J. H. Connor, G. Shvets, H. Altug, *Proc. Natl. Acad. Sci. USA* **2011**, *108*, 11784.
[13] D. Franklin, Y. Chen, A. Vazquez-Guardado, S. Modak, J. Boroumand, D. Xu, S.-T. Wu, D. Chanda, *Nat. Commun.* **2015**, *6*, 1.
[14] P. R. West, S. Ishii, G. V. Naik, N. K. Emani, V. M. Shalaev, A. Boltasseva, *Laser Photonics Rev.* **2010**, *4*, 795.
[15] A. Kristensen, J. K. W. Yang, S. I. Bozhevolnyi, S. Link, P. Nordlander, N. J. Halas, N. A. Mortensen, *Nat. Rev. Mat.* **2016**, *2*, 16088.
[16] A. V. Yakovlev, V. A. Milichko, V. V. Vinogradov, A. V. Vinogradov, *Adv. Funct. Mater.* **2015**, *25*, 7375.
[17] Q. Chen, X. Hu, L. Wen, Y. Yu, D. R. S. Cumming, *Small* **2016**, *12*, 4922.
[18] L. Duempelmann, B. Gallinet, L. Novotny, *ACS Photonics* **2017**, *4*, 236.
[19] N. C. Lindquist, P. Nagpal, K. M. McPeak, D. J. Norris, S.-H. Oh, *Rep. Prog. Phys.* **2012**, *75*, 036501.
[20] B. J. de Gans, P. C. Duineveld, U. S. Schubert, *Adv. Mater.* **2004**, *16*, 203.
[21] H. Zollinger, *Color Chemistry*, John Wiley & Sons, Hoboken, NJ, USA, **2003**.
[22] P. Galliker, J. Schneider, H. Eghlidi, S. Kress, V. Sandoghdar, D. Poulikakos, *Nat. Commun.* **2012**, *3*, 890.
[23] J. Y. Kim, C. Ingrosso, V. Fakhfouri, M. Striccoli, A. Agostiano, M. L. Curri, J. Brugger, *Small* **2009**, *5*, 1051.
[24] P. Richner, P. Galliker, T. Lendenmann, S. J. P. Kress, D. K. Kim, D. J. Norris, D. Poulikakos, *ACS Photonics* **2016**, *3*, 754.
[25] A. V. Yakovlev, V. A. Milichko, V. V. Vinogradov, A. V. Vinogradov, *ACS Nano* **2016**, *10*, 3078.
[26] L. Rayleigh, *Philosophical Magazine Series 6*, Vol. *14*, Taylor & Francis online, **1907**, p. 60.
[27] D. Maystre, *Prog. Opt.* **1984**, *21*, 1. x) D. Maystre. Theory of Wood's anomalies, *Plasmonics*. Springer Berlin Heidelberg, Heidelberg, Germany.
[28] M. D. Fairchild, *Color Appearance Models*, John Wiley & Sons, Ltd, Chichester, UK, **2013**.
[29] X. Zhu, C. Vannahme, E. Hølund-Nielsen, N. A. Mortensen, A. Kristensen, *Nat. Nanotechnol.* **2015**, *11*, 325.
[30] W. Qiao, W. Huang, Y. Liu, X. Li, L.-S. Chen, J.-X. Tang, *Adv. Mater.* **2016**, *28*, 10353.
[31] T. D. James, P. Mulvaney, A. Roberts, *Nano Lett.* **2016**, *16*, 3817.
[32] A. S. Roberts, A. Pors, O. Albrektsen, S. I. Bozhevolnyi, *Nano Lett.* **2014**, *14*, 783.
[33] M. G. Moharam, T. K. Gaylord, *J. Opt. Soc. Am.* **1981**, *71*, 811.

 

ADVANCED OPTICAL MATERIALS

# Supporting Information

for *Advanced Optical Materials,* DOI: 10.1002/adom.201700153

# Controlling the Color of Plasmonic Substrates with Inkjet Printing

*Luc Duempelmann, Judith A. Müller, Fabian Lütolf,* Benjamin Gallinet, Rolando Ferrini, and Lukas Novotny*

Submitted to ADVANCED OPTICAL MATERIALS

# Supporting Information

for *Adv. Opt. Mater.*, DOI: 10.1002/adom.201700153

**Title** Controlling the Color of Plasmonic Substrates with Inkjet Printing

*Luc Duempelmann, Judith A. Müller, Fabian Lütolf*, Benjamin Gallinet, Rolando Ferrini, and Lukas Novotny*

## 1. Coating with Low-Refractive Ink

The viscosity of the low refractive index ink ($n_{coat}$ = 1.33) was too high for inkjet printing. Therefore it was finally spin coated onto the sample. **Figure S1** clearly shows that coating of this ink changes the optical property of the other inks only very little. Therefore this process can be utilized to add the third ink onto the substrate without changing the color effect of the other inks. Finally, this embedding protects the sample.

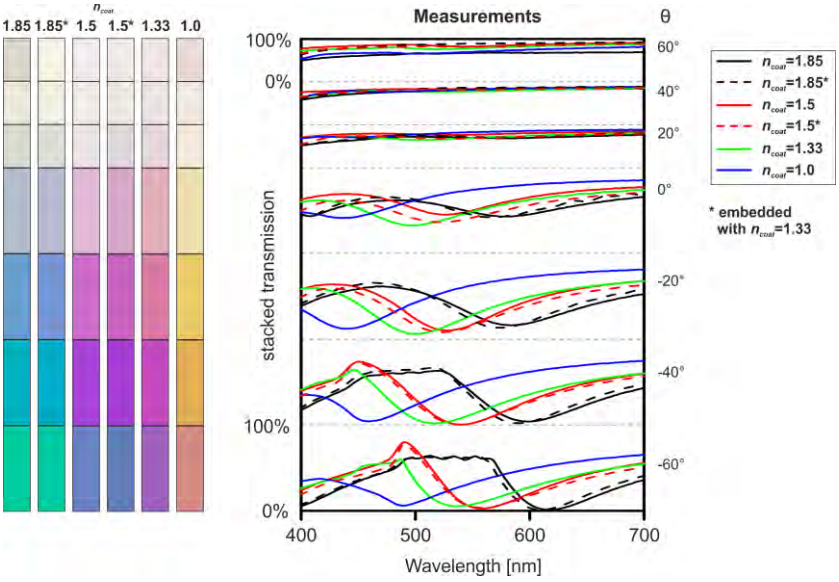


**Figure S1.** Measured transmission spectra of TM-polarized light for different angles θ and RI-inks (colored lines and bold numbers). The * indicates the already printed RI-inks which were finally embedded with a RI-ink of $n_{coat}$ = 1.33.

## 2. Geometrical Influence onto the Resonance

**Figure S2** shows the effect of geometrical parameters e.g. filling factor of $n_{coat}$ or period) onto the resonance. Structures with more $n_{coat}$ around the plasmonic structure are more effected by the RI of the ink. This is illustrated by the slope of the LSPR (indicated at minimum position), see Figure S2a-c. The greatest change (highest slope) is achieved with freestanding structures, which are more difficult to fabricate. If the structures are nearly completely surrounded by $n_{sub}$ (see Figure S2c) the effect is rather small. Figure S2d shows the effect of the LSPR on the shape of the resonance. The period mainly effects the position of the propagating resonance, indicated by WR (see Figure S2e-g). Smaller period leads to a blueshift. Separation of the WR and LSPR leads to a decrease in the strong coupling of the two resonances. This can be see by the broadening of the LSPR and a flattening of the Fano like lineshape, see Figure S2h.

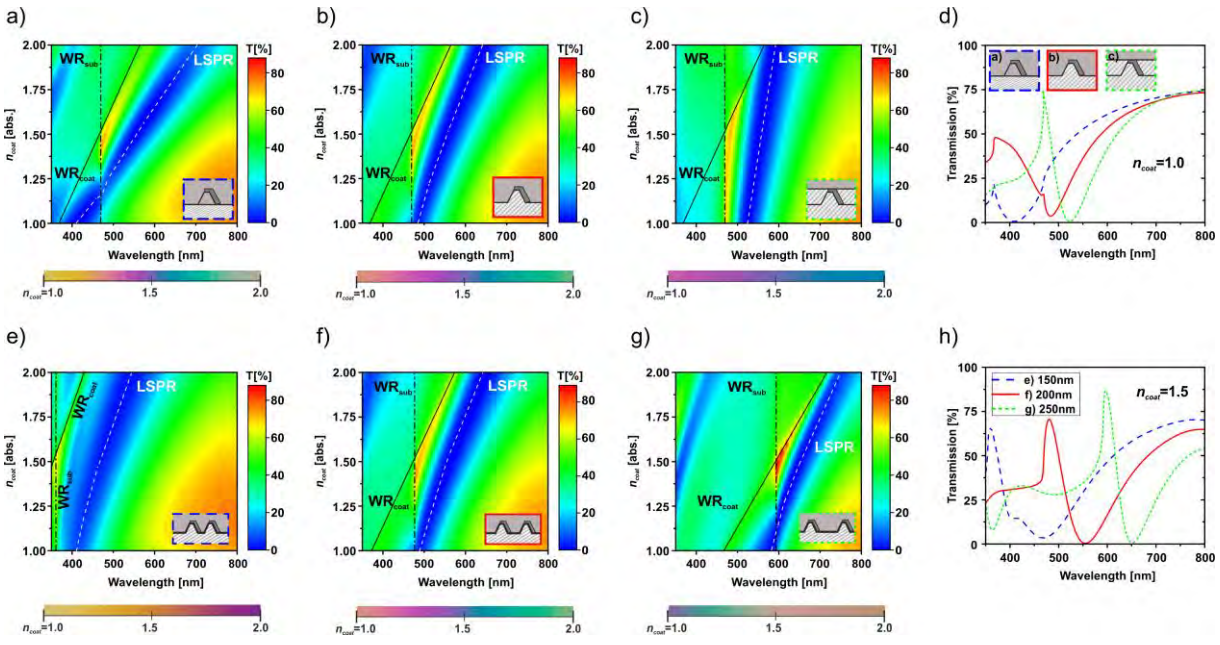


**Figure S2.** Simulated transmission spectra as a function of $n_{coat}$ = 1.0-2.0 at θ = -60°. (a-c) varying percentage of $n_{coat}$ compared to the layer with (a) ~91%, (b) ~64% and (c) 0%. The corresponding position of the LSPR's are used in Figure 3b. (e-g) varying period of the structure with (d) p = 150 nm, (e) p = 200 nm and (f) p = 250 nm. (d) shows the spectra of (a-c) at $n_{coat}$ = 1.0; (h) similar from (e-g) at $n_{coat}$ = 1.5. Figure 7 (b,e) corresponds to Figure 3 (a).

## 3. Mixing different RI-Inks

**Figure S3** illustrates how more colors can be generated by mixing different RI-inks. Figure S3a shows the color generation of increasing the ratio of $n_{coat}$ = 1.85 to $n_{coat}$ = 1.0. This can be realized by printing the coating ($n_{coat}$ = 1.85) several times with a low surface coverage (uncovered pixels), see Figure S3b. Such kind of mixing can be done with basically any kind of RI-inks present on the white line. Figure S3c illustrates the potential mixing of the four demonstrated basic colors (crosses) including color bars, see Figure S3d.

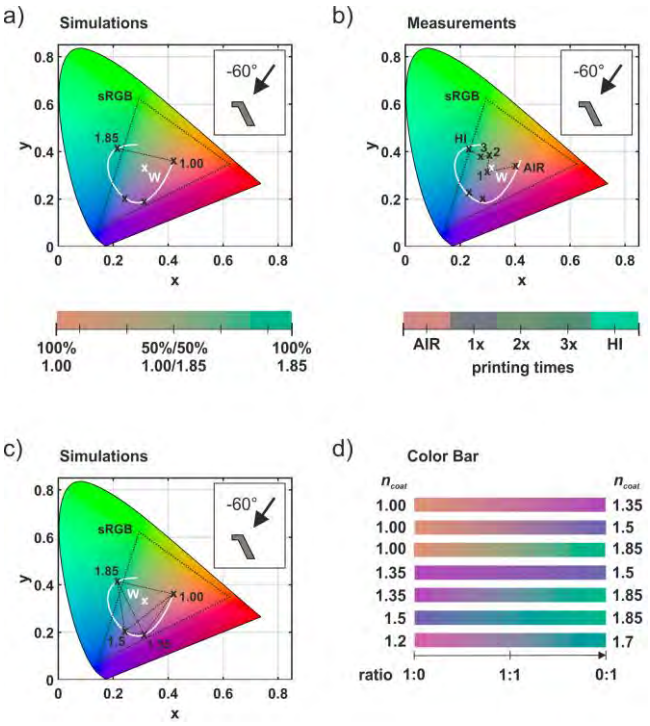


**Figure S3.** (a-c) CIE color plots for $n_{coat}$ = 1.0-2.0 (white line) at θ = -60°. (a) Simulated mixing of $n_{coat}$ = 1.0 and $n_{coat}$ = 1.85. (b) Experimental realization of (a) by multiple printing of $n_{coat}$ = 1.85 (indicated as crosses). (c) Simulated mixing of RI-inks with (d) corresponding color bars. The sRGB color range is indicated by the dashed triangle.

## 4. Comparison before and after Inkjet Printing

**Figure S4** illustrates the color change induced by inkjet printing of $n_{coat}$ = 1.85 (building and the lower part of background) and $n_{coat}$ = 1.5 (car at the bottom and upper part of the background) onto the plasmonic substrate. The substrates features inhomogeneity (see top), which is caused by the replication and the evaporation process. These slight color changes are however hardly noticeable in the presence of the much stronger coloration induced by printing.

a) before printing

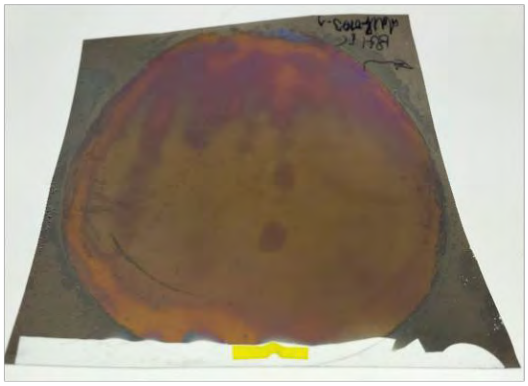

b) after printing

**Figure S4.** Comparison of a plasmonic substrate (a) before and (b) after inkjet printing.